land

MDPI

Article

Spatial and Temporal Heterogeneity of Eco-Environmental Quality in Yanhe Watershed (China) Using the Remote-Sensing-Based Ecological Index (RSEI)

Lingda Zhang [1], Quanhua Hou [1,2,*], Yaqiong Duan [1,2,*] and Sanbao Ma [3]

[1] School of Architecture, Chang'an University, Xi'an 710061, China; zhangld@chd.edu.cn
[2] Engineering Research Center of Collaborative Planning of Low-Carbon Urban Space and Transportation, Universities of Shaanxi Province, Xi'an 710061, China
[3] Suide Soil and Water Conservation Scientific Experimental Station of Yellow River Water Conservancy Commission, Yulin 719000, China; msb0324@163.com
* Correspondence: houquanhua@chd.edu.cn (Q.H.); duanyaqiong@chd.edu.cn (Y.D.)

Abstract: The long-term impacts of climate change and human activities have resulted in the Yanhe watershed, a typical watershed in the Loess Plateau region, exhibiting a high degree of vulnerability and significant heterogeneity in ecological environmental quality. This has led to environmental degradation and complex socio-ecological challenges. Consequently, there is an urgent need to carry out research on the spatial and temporal differentiation patterns of ecological environment quality. By utilizing remote sensing data spanning 21 years, this study evaluated the evolutionary trends and consistency of ecological environment quality (EEQ) within the Yanhe watershed based on the remote-sensing-based ecological index (RSEI). Furthermore, it examined global and local spatial autocorrelation of the RSEI by constructing a hexagonal grid, thereby revealing the spatiotemporal characteristics of EEQ at different scales within the Yanhe watershed. The results were as follows: (1) The EEQ has exhibited an overall upward trend in the past two decades, while it has displayed significant fluctuations; (2) the Global Moran's I values for the years 2000, 2010, and 2020 were 0.18, 0.32, and 0.21, respectively, indicating a presence of spatial autocorrelation within the RSEI; (3) the overall EEQ of the Yanhe watershed will continue to improve, although the ecological quality in certain areas remains unstable due to local natural conditions and human activities. This research not only contributes to the technical framework for analyzing the spatiotemporal heterogeneity of EEQ but also provides actionable insights for ecosystem restoration and sustainability within the Loess Plateau watershed. Our work advances the understanding of ecological dynamics in semi-arid regions and offers a model for assessing ecological quality in similar environmental contexts.

Keywords: Google Earth Engine; Yanhe watershed; RSEI; time–space analysis; hexagonal grid

check for updates

Citation: Zhang, L.; Hou, Q.; Duan, Y.; Ma, S. Spatial and Temporal Heterogeneity of Eco-Environmental Quality in Yanhe Watershed (China) Using the Remote-Sensing-Based Ecological Index (RSEI). *Land* **2024**, *13*, 780. https://doi.org/10.3390/land13060780

Academic Editors: Guillermo J. Martinez-Pastur, Wei Song, Cong Ou, Jieyong Wang, Yaqun Liu, Kangwen Zhu and Xuanchang Zhang

Received: 21 March 2024
Revised: 28 May 2024
Accepted: 29 May 2024
Published: 31 May 2024

Copyright: © 2024 by the authors. Licensee MDPI, Basel, Switzerland. This article is an open access article distributed under the terms and conditions of the Creative Commons Attribution (CC BY) license (https://creativecommons.org/licenses/by/4.0/).

1. Introduction

As the earth enters the Anthropocene [1], the functions and spatial patterns of surface ecosystems are undergoing drastic changes that resulted from the combined influences of climate change and human activities. Consequently, numerous social and ecological environmental issues are emerging, including urban heat island [2,3] and rain and flood damage [4], and the loss of biodiversity and the fragmentation of ecological tableland have severely impacted the local ecological environment quality (EEQ) and sustainable development. In the process of urbanization together with rapid population growth, construction land is expanded in a disorderly fashion and natural resources are consumed excessively, which greatly disrupt ecosystem functions at various scales and threaten the living environment. The Chinese government has proposed an ecological civilization construction strategy, under which background ecological-protection-oriented sustainable development has become the core goal of high-quality regional development in China.

Despite the implementation of numerous environmental protection policies and plans, certain areas with weak ecological background conditions and lagging social and economic development still exhibit unstable EEQ and poor sustainability [5].

The Loess Plateau is one of the most eroded regions in the world [6]. As a major ecological barrier in China, it not only has long faced tremendous environmental problems and low ecological resilience but has also been caught in a complex and conflicting man–earth relationship. To address these contradictions, the Chinese government has implemented several initiatives on the Loess Plateau, including the Grain-for-Green Program (GFG) and the Gully Land Consolidation (GLG), which restored cropland to forest or grassland, as well as renovated and efficiently used the stable gullies [7]. As the fruits of the GFG program, 16,000 km^2 of rain-fed farmland were converted into forest or grassland during 1999 and 2010 [8]. Although these projects have achieved remarkable results, according to recent studies, the ecological environment in the Loess Plateau is becoming gradually saturated and has even led to ecological degradation in some areas [9]. In the Loess Plateau region, the change in ecological quality is influenced not only by climate-change-related factors such as temperature and precipitation [10,11], but also by socioeconomic factors such as the expansion of construction land and population migration driven by urban–rural development [12,13]. Although the techniques and methods for the ecological quality assessment are relatively mature, challenges remain in data acquisition, indicator selection, and conducting long-term dynamic assessments. Therefore, there is an urgent need to establish a more comprehensive ecological quality assessment indicator system and utilize remote sensing data to monitor the long-term series of ecological changes at various spatial scales [14,15].

The remote sensing technology contributes to the effective, scientific support for large-scale and long-term ecosystem monitoring. In recent years, many scholars have used different algorithms to detect and evaluate the ecological environment of forests, grasslands, rivers, and lakes, including the NDVI index [16], primary net productivity [17], carbon sequestration [18,19], humidity [20], and others. These indicators can reflect the regional ecological environment state from different perspectives, particularly when examined over long-term time-series data, and were widely adopted in various ecological studies. However, because there are diverse complex influencing factors, relying solely on a single ecological indicator is insufficient for assessing the state of an ecosystem [21]. Recently, the remote-sensing-based ecological index (RSEI), that combines the indicators of Greenness, Wetness, Dryness, and Heat, has been put forward for assessing the spatial–temporal variations in ecological changes by Xu [14]. The RSEI is based on the four key ecological elements, and the principal component analysis (PCA), based on covariance, serves to determine the end. Subsequently, the ecological index is calculated. Through the aggregation of multiple indicators, the RSEI has overcome the limitation of reflecting regional ecological quality by a single ecological index in the past and has been widely used in regions with unique climatic conditions [13,15,22,23].

At present, the RSEI-based temporal dynamic change characteristics of EEQ can be broadly categorized into two aspects. The first is the analysis of the characteristics of time dynamic changes, which is mainly based on the linear regression analysis, Theil–Sen slope analysis, and Mann–Kendall trend analysis, and the latter two are non-parametric tests with no assumptions needing to be satisfied. Their combination confirms the time-series data (TSD) trend and allows the significance tests. The method is a common non-parametric statistical method for the processing of hydrological series data and meteorological data, and is widely used in the EEQ long-term trend analysis [24–26]. Second, it is based on long-term data to evaluate the future trend of change and simulate different scenarios, such as the R/S analysis [27] and the CA-Markov model [13]. The former is originally proposed by Hurst [28] to measure the change in trend intensity and noise level over time. Due to the robustness of its algorithm, it has been widely used in the analysis of long-term time-series data [29,30], and can be effectively used to analyze the consistency of the space–time evolution of the ecological index. Therefore, the integration of these two

analytical approaches can provide a more comprehensive examination of the patterns and future trajectories pertaining to quality.

However, only focusing on the spectral features or evaluation index system of remote sensing data is insufficient to explain the regional background information and spatial characteristics reflected in the data [31]. Spatial autocorrelation is a common method to explain the spatial relationships and features of elements, which is conducive to further mining the spatial distribution characteristics of the RSEIin a certain period, including global autocorrelation and local autocorrelation, and is suitable for measuring whether the distribution of spatial variables has aggregation. The RSEI, as a comprehensive spatial representation of regional ecological environment quality, has the characteristics of spatial dependence [32], especially in regions with large ecological environment differences. The RSEI has been applied in a relatively mature way in river basins [33,34], cities [35], urban agglomerations [36], mountain areas [37], etc. However, there has been limited focus on micro or local scales, and the change characteristics of the multi-scale RSEI have often been overlooked. Some scholars have carried out spatial correlation research on the RSEI based on the 1 km × 1 km, 600 m × 600 m, and grid scale [21,38], yielding more accurate results.

Considering the reliability and extensive applicability of the RSEI, a multi-level analysis approach toward temporal and spatial dimensions can be further developed to investigate the dynamics of regional ecological environment quality. Moreover, integrating a grid analysis enables the more precise identification of ecological environment quality across various scales. Therefore, the Yanhe watershed was used as the research area, and the RSEI was constructed by integrating NDVI, WET, LST, and NDBSI. And the Sen + Mann–Kendall model and Hurst Exponent were selected for analyzing the changing trend and sustainability of EEQ in the Yanhe watershed. The global and local spatial autocorrelation analysis was based on the division of the hexagonal grid, to identify the spatiotemporal characteristics of EEQ in the Yanhe watershed. Our objective is to (1) analyze the intensity of the EEQ change in the Yanhe watershed between 2000 and 2020, (2) investigate the characteristics, trends, and sustainability of dynamic changes in the RSEI long-term series using the Sen + Mann–Kendall method and Hurst Exponent, and (3) analyze the spatial autocorrelation regarding the RSEI at different scales.

2. Materials and Methods

2.1. Study Area

The Yanhe, the principal tributary of the Yellow River, originates in the southern foothills of Baiyu Mountain and traverses the central region of the Loess Plateau. It flows from northwest to southeast through Jingbian County, Zhidan County, Ansai District, Baota District, and Yanchang County, before joining the Yellow River near Liangshui'an village in Yanchang County. It is situated within a geographical framework of 36°21′ to 37°19′ N latitude and 108°38′ to 110°29′ E longitude, and spans an area of approximately 7758 km^2 (Figure 1). The landform in the basin is dominated by hills and gullies. The terrain is high in the northwest and low in the southeast, featuring a broken and undulating topography, and is fully Id, illustrating the regularity of spatial differentiation inherent to the geomorphology of this region. In Yanhe watershed, the average density of gullies is 475 km/km^2, placing it in the second sub-region of the Loess hilly and gully region, and serves as a quintessential exemplar of this region. The watershed experiences a semi-arid monsoon climate on the plateau, with average annual rainfall ranging from 400 to 500 mm. The soil type is mainly yellow spongy soil [39] which is a typical watershed unit in the Loess Plateau. As the GFG program has been implemented in recent decades, the land use pattern of Yanhe watershed has undergone significant changes. The scale of forest and grassland has increased, the amount of slope cultivated land has sharply decreased, and the ecological environment has been improving day by day [40]. However, some studies have shown that the unreasonable temporal and spatial position of ecological engineering, such as irrational land use and indiscriminate conversion of farmland to forests, along with other human activities [8,41], may cause ecological degradation in local areas. As a result, the vegetation may respond to

the climate change and human interventions in a delayed and complex manner. Meanwhile, in the process of urbanization and agricultural modernization, the ecological environment has become more complex. The continuous interference with the ecological environment presents significant challenges to the sustainability of the ecological environment in the Yanhe watershed face. These drastic changes in social and ecological spatial patterns make the Yanhe watershed an ideal setting to study the relationship between EEQ and human activities and its management measures [39].

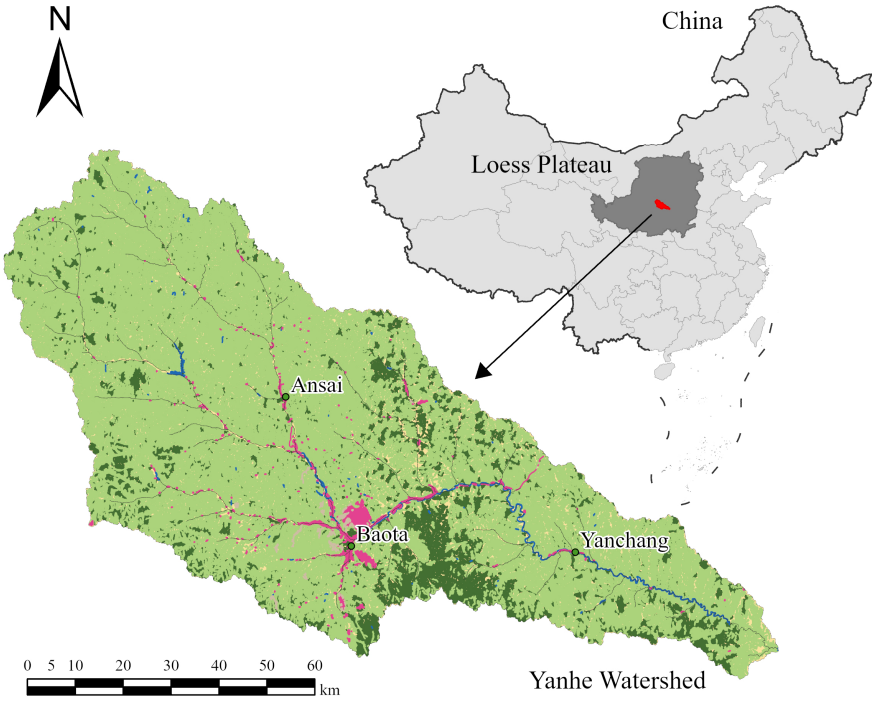


Figure 1. Location of study area.

2.2. Data Sources and Pre-Processing

Landsat5 TM, Landsat7 ETM+, and Landsat8 OLI/TIRS images served for calculating the RSEI from 2000 to 2020 at 30 m resolution using the GEE platform (http://www.usgs.gov, accessed on 20 April 2023). Considering the errors generated by the image data and the seasonal images of local vegetation, this study, combined with the local actual situation, selected the months with stable vegetation cover changes in the Yanhe watershed, from May to October [42], and controlled the cloud cover within 10%. Meanwhile, the Landsat series surface reflectance data underwent radiometric, atmospheric, and geometric accuracy corrections on the GEE platform under the assistance of a Python3.11 script API. We adopted the normalized difference water index (MNDWI) for masking the water bodies, aiming at avoiding the impact of the large water areas on the calculation of RSEI [43].

Due to the accuracy of the research data and based on the reference of related research [44], this study selected a 4 km^2 hexagonal grid as the basic research unit for exploring the spatial variation of RSEI in the Yanhe watershed. Compared to a rectangular grid, the hexagonal lattice provides a simpler, better-aligned nearest neighborhood and better visualization effect [45]. These properties allow hexagons to better describe and simulate spatial relationships between objects.

2.3. Methods

This study establishes a spatiotemporal analysis methodology for assessing the quality of regional ecological environments, comprising two main components: computation of the RSEI using the GEE platform, and conducting trend analysis and spatial autocorrelation analysis on raster data using the ArcGIS10.8 platform (Figure 2).

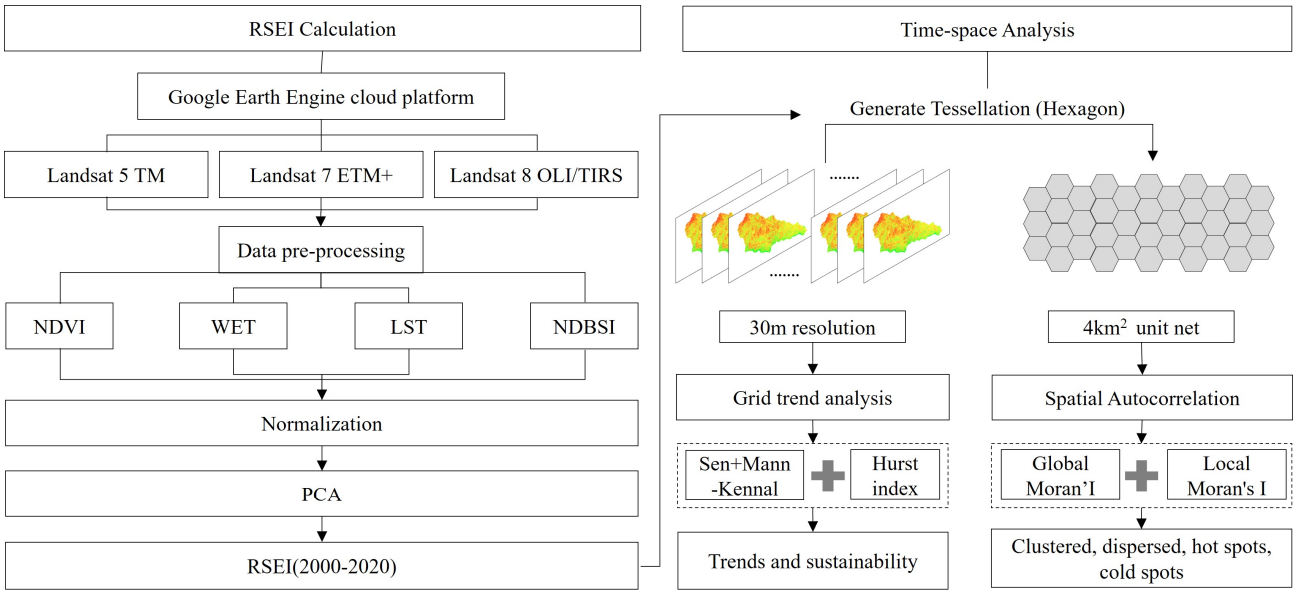


Figure 2. Research workflow.

2.3.1. RSEI Calculation

This study used the RSEI for monitoring the ecological environment quality fluctuations in Yanhe watershed during 2000 and 2020. RSEI was coupled with four evaluation indices, including NDVI, WET, NDBSI, and LST, representing Greenness, Wetness, Heat, and Dryness. And the first principal component (PCA1) was extracted by principal component analysis (PCA) based on GEE platform. The calculation formula is:

$$RSEI = PCA1[f(NDVI, WET, NDBSI\ LST)] \quad (1)$$

The NDVI denotes the indicator Greenness, exhibiting a close association with plant biomass, leaf area index, and vegetation cover [16]. In general, a higher NDVI value indicates better vegetation growth and development, which can, to some extent, reflect the regional EEQ [46].

The Wet index is calculated using the Tassel Cap Conversion Tool and is expressed as the moisture component, reflecting the moisture levels regarding water, soil, and vegetation, and showing a close association with the regional ecological environment. The calculation formulae for Landsat TM/ETM+/OLI images can be found in references [47–49].

The index-based built-up index (IBI) widely serves for accurately mapping built-up areas [46]. There are also bare lands or lands with sparse vegetation at the sites cut down or abandoned throughout the study area, which are represented by a soil index (SI). Hence, we used the index NDBSI, which combined IBI and SI.

The Heat index is calculated by land surface temperature (LST). Landsat TM/ETM+ thermal band 6 and Landsat OLI thermal band 10 served for the land surface temperature inversion [50].

Subsequently, our study adopted the PCA method, combining the 4 metrics for forming RSEI, which was represented by the first component of PCA. Generally, it falls into five grades linearly (interval: 0.2), namely, Bad (0–0.2), Poor (0.2–0.4), Moderate (0.4–0.6), Good (0.6–0.8), and Excellent (0.8–1.0), thereby enabling a qualitative description of the ecological conditions [14].

2.3.2. Sen + Mann–Kendall Analysis

Sen's slope, a non-parametric analytical tool, is particularly adept at examining time-series data (TSD) that are characterized by independence and robustness to anomalies and missing values [51]. The method ascertains the trend direction through the calculation of

the median difference between sequential data points. A positive slope is indicative of an upward trend, whereas a negative slope points towards a downward trend.

Lacking a direct statistical significance test for the TSD trend, the Mann–Kendall test has been adopted to assess the significance of the trend [52,53]. This non-parametric statistical technique is well-suited for multidimensional TSD and demonstrates resilience in the presence of outliers. The test employs a signum function to ascertain the trend's direction. With an ample sample size ($n > 10$), the resulting test statistic converges to a standard normal distribution, thereby facilitating hypothesis testing through the computation of the Z-score.

2.3.3. Hurst Exponent

The Hurst Exponent [28] can reflect the self-similarity and long-term dependence of long-term time-series data and is used to describe the future pixel-by-pixel change trend of the study area. Utilizing the R/S (Range/Standard Deviation) analysis method, we derived the H value, which delineates three distinct types of series behavior: anti-persistence ($H < 0.5$), where past fluctuations do not influence future trends; a random walk ($H = 0.5$), indicating no correlation between past and future states; and positive persistence ($H > 0.5$), where past movements tend to be followed by similar changes, suggesting a trend continuity. This classification enhances the interpretability of the study's temporal dynamics analysis.

2.3.4. Spatial Autocorrelation Analysis

The study leverages the Global Moran's I and Local Moran's I indices to analyze the spatial correlation of RSEI. These indices reveal the geographic concentration of ecological conditions within the Yanhe watershed and identify local spatial patterns. The Global Moran's I index reflects the overall spatial heterogeneity, while the Local Moran's I, along with Moran scatter plots, uncovers the local aggregation and dispersion characteristics of RSEI, differentiating between high–high (H–H), low–low (L–L), high–low (H–L), and low–high (L–H) spatial units.

3. Results

3.1. RSEI-Based Ecological Environment Evaluation

From 2000 to 2020, the load of greenness and humidity is positive among the four indicators (Table 1). The average humidity of 0.52 is slightly higher than the average greenness of 0.50, revealing the larger contribution made by humidity to the RSEI in the Yanhe watershed. On the other hand, the load of heat and dryness is negative, and the average dryness load has an absolute value of 0.53, higher than that of heat, which is 0.44. This observation aligns with the actual conditions in the Yanhe watershed. Moreover, the four indicators achieved an average contribution rate of 82.70% in the first principal component (PC1); the highest value in 2014 was 89.96%, and the lowest was 73.38% in 2000. This demonstrates that more than 80% of the index information features are concentrated on PC1. Hence, it is practical to build the RSEI based on PC1 in the Yanhe watershed, avoiding the result bias caused by the subjective weighting in the process of calculation.

3.2. Analysis of Temporal Dynamic Change of EEQ

3.2.1. Analysis of the Overall Change in RSEI

Figure 3 provides a comprehensive graphical overview of the mean change statistics in the RSEI within the Yanhe watershed from 2000 to 2020. The trend line depicted in the figure illustrates the overall upward trajectory of the RSEI, indicative of the improving ecological environment quality (EEQ) over the two-decade period. Notably, the figure also highlights significant fluctuations, especially post-2010, which can be attributed to the interplay between climate change impacts and human activities, such as urbanization, and agricultural and ecological practices. The peak in the RSEI mean value observed in 2018

corresponds with the year that exhibited the highest proportion of areas classified under the 'excellent' category of EEQ, as shown in Figure 4.

Table 1. Result of principal component analysis during 2000–2020.

Year	Loading of NDVI	Loading of WET	Loading of LST	Loading of NDBSI	Percentage of Covariance Eigenvalue of PC1 (%)
2000	0.48	0.55	−0.44	−0.52	73.38
2001	0.47	0.55	−0.45	−0.52	74.32
2002	0.48	0.53	−0.47	−0.53	81.14
2003	0.46	0.52	−0.5	−0.51	81.83
2004	0.51	0.51	−0.45	−0.52	84.05
2005	0.51	0.52	−0.44	−0.53	80.11
2006	0.50	0.49	−0.48	−0.53	78.81
2007	0.49	0.55	−0.40	−0.54	81.97
2008	0.51	0.51	−0.46	−0.52	83.85
2009	0.52	0.53	−0.39	−0.54	76.06
2010	0.52	0.53	−0.39	−0.54	84.00
2011	0.49	0.52	−0.49	−0.51	76.85
2012	0.49	0.51	−0.47	−0.52	86.12
2013	0.49	0.51	−0.45	−0.54	83.46
2014	0.5	0.51	−0.44	−0.54	89.96
2015	0.53	0.52	−0.42	−0.53	85.52
2016	0.52	0.5	−0.44	−0.53	88.75
2017	0.53	0.52	−0.41	−0.53	84.69
2018	0.53	0.51	−0.37	−0.57	87.04
2019	0.51	0.50	−0.47	−0.52	87.6
2020	0.53	0.50	−0.44	−0.53	87.09
Mean	0.50	0.52	−0.44	−0.53	82.70

Figure 4 delineates the temporal shifts in the distribution of EEQ categories within the Yanhe watershed over the past two decades. The analysis reveals a relatively stable trend for areas classified as 'poor' and 'excellent' in terms of EEQ, whereas the proportions of the 'bad', 'medium', and 'good' categories display more considerable fluctuations. From 2000 to 2020, the 'excellent' grade demonstrates a slight overall reduction, dropping from 12.33% to 11.01%. A more pronounced fluctuation is observed between 2014 and 2020, with a notable peak at 21.86% in 2018. This peak coincides with the year that recorded the highest mean RSEI, as detailed in Figure 3. By 2020, the proportion of 'excellent' areas decreases to 10.35%. Significantly, the proportion of areas with 'good' EEQ undergoes a substantial increase, rising from 11.84% in 2000 to a high of 31.05% in 2018, and settling at 18.95% by 2020. In contrast, the 'poor' category maintains minimal fluctuations throughout the study period. The 'bad' category exhibits the most significant oscillations, with its proportion dropping sharply from 29.14% in 2000 to 15.91% by 2013. A slight rebound is observed in the subsequent four years, culminating in a low of 6.72% in 2018. While the general trend indicates a gradual improvement towards better EEQ, the Yanhe watersheds' ecological state is marked by instability and vulnerability. The fluctuations observed in certain categories underscore the dynamic interplay of ecological recovery efforts and the pressures of environmental change. It shows the changing process of the proportion of different EEQ horizontal areas in the Yanhe watershed in the recent 20 years (Figure 4).

In alignment with the socio-economic development trajectory of the Yanhe watershed, Figure 3 underscores that the ecological environment quality (EEQ) has undergone notable variations since the year 2010. To capture these dynamics, our analysis is segmented into three distinct chronological phases—years 2000, 2010, and 2020—to provide a focused examination of the spatiotemporal distribution of the RSEI.

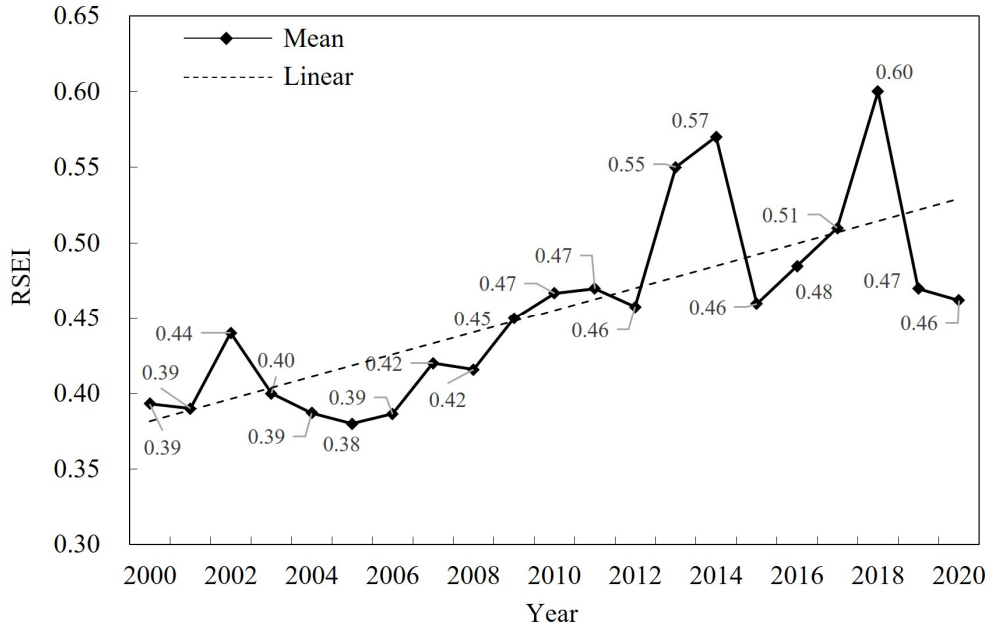


Figure 3. RSEI mean change statistics from 2000 to 2020.

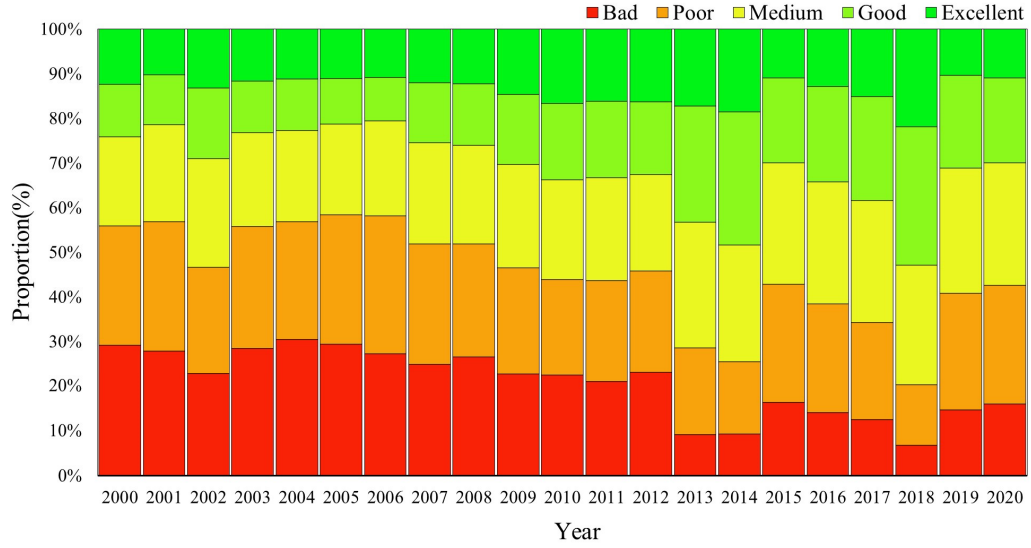


Figure 4. Changes in ecologic environment grade in Yanhe watershed from 2000 to 2020.

Figure 5 offers a comparative spatial distribution of the RSEI across these benchmark years. In the year 2000, regions classified as 'excellent' and 'good' were predominantly located in the southern mountainous zones and the vicinity of the main watercourse of the Yanhe watershed. A decade later, in 2010, there was a marked enhancement in the RSEI across the central and southern sectors, indicative of an overall improvement in EEQ. Nevertheless, a decline in the RSEI was observed in certain areas of the northwest region, suggesting a gradient of ecological responses to local conditions. By 2020, the RSEI in the southern region had maintained its stability, while a significant expansion in the distribution of high RSEI values was noted in the upper reaches. Conversely, an increase in low RSEI values was detected in the middle reaches, particularly within the middle and upper segments of the watershed. When compared to the data from 2000, the aggregate proportion of areas with 'excellent' and 'good' RSEI ratings had increased by 2020. However, a distinct clustering of low RSEI values in specific locales suggests the presence of ecological challenges that require targeted interventions.

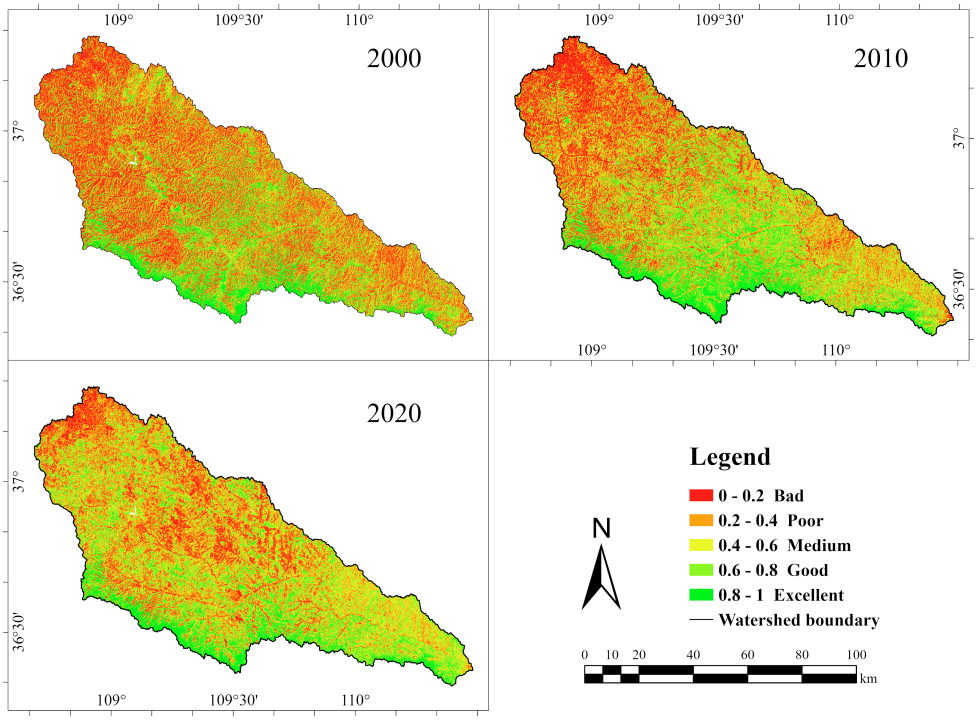


Figure 5. 2000–2020 spatial distribution of RSEI quality levels in the Yanhe watershed.

3.2.2. RSEI Trend Analysis

(1) RSEI dynamic trend during 2000–2020

Figure 6 shows trends in the RSEI by the Sen + Mann–Kendall method from 2000 to 2020 in the Yanhe watershed. The classification of trends is based on the direction of change (increase or decrease) and the level of statistical significance [26]. For the purpose of this study, a significance level of 0.01 was selected to distinguish between significant and non-significant trends. Significant trends were further differentiated into 'Highly Significant' and 'Significant' to reflect the rigor of the statistical test. As can be seen from the figure, the trend of the RSEI in the Yanhe watershed shows a high spatial heterogeneity. Over the past 20 years, the 72.48% of the watershed has essentially remained unchanged, with an area of about 5569.39 km^2, primarily distributed in the upper, middle, and lower reaches of the southern mountains. The reduction area is approximately 179.48 km^2, accounting for only 2.34%, part of the area mainly distributed in the middle and lower reaches of the urban construction-intensive area and the perimeter of major roads. And other parts appear in the north and south of the watershed with a complex terrain. Most visibly, the area with the highly significant reduction is about 96.88 km^2, which is mainly distributed near the central urban area of Baota District, indicating that urbanization in recent years has significantly impacted the ecological environment. The RSEI increase value is 1935.65 km^2, accounting for a total of 25.19%, with a wide distribution range, on the middle and upper reaches of the watershed (Table 2). The higher increase area was mainly gathered in both sides of the main river channels of the Yanhe watershed, which is closely related to the ecological restoration projects in recent years.

(2) Consistency of future RSEI trend

To further analyze the consistency of the RSEI change trend, the R/S analysis was used to calculate the Hurst Exponent pixel by pixel to obtain the sustainable spatial distribution of the RSEI change trend in the Yanhe watershed. The Hurst Exponent's overall threshold ranges from 0.06 to 0.99, with an average of 0.69. In Figure 7, the area with a Hurst Exponent higher than 0.5 accounts for 88.66% of the entire watershed, which is widely distributed and mainly concentrated in the upper and middle reaches and lower reaches of the watershed, indicating that the future RSEI change trend of the Yanhe watershed will be consistent with

the changing trend from 2000 to 2020. That is, the RSEI will be on the rise in the future, and the EEQ will be improved continuously. The proportion of regions with a Hurst Exponent lower than 0.5 is 10.96%, mainly found in the middle and upper reaches, indicating that the RSEI of this region presents anti-sustainability, and the EEQ will decline in the future. Furthermore, the region with a Hurst Exponent equal to 0.5 is only 0.37%. Therefore, on the whole, the EEQ change in the Yanhe watershed in the future has a trend of improvement, and sustainability is strong.

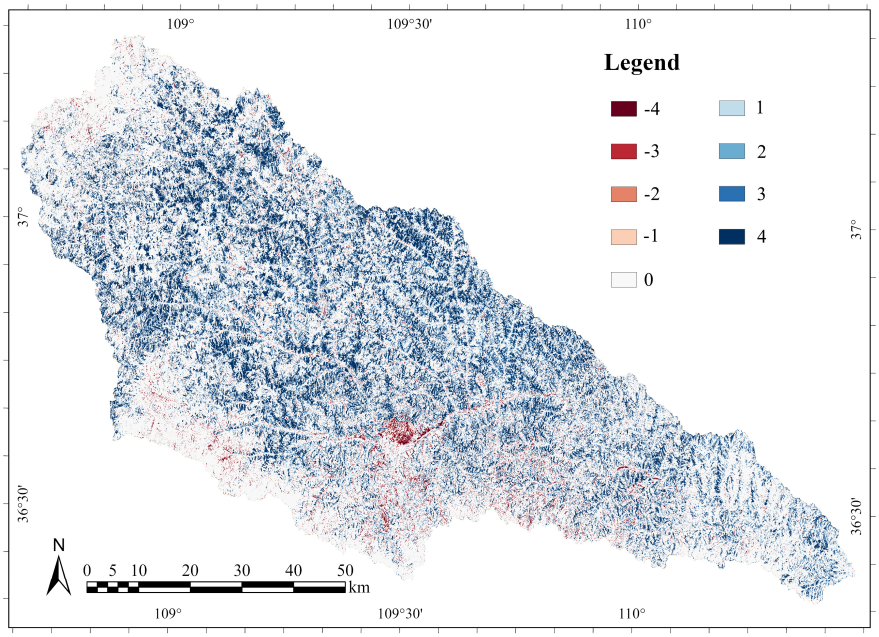


Figure 6. RSEI trend classification in Yanhe River Basin from 2000 to 2020.

Table 2. Classification statistics of RSEI change trend in Yanhe watershed from 2000 to 2020.

Trend Classification	Trend Features	Area	Proportion
−4	Highly significant reduction	96.88	1.26%
−3	Significant reduction	63.91	0.83%
−2	Slightly significant reduction	13.45	0.18%
−1	Non-significant reduction	5.24	0.07%
0	Unchanged	5569.39	72.48%
1	Non-significant increase	15.51	0.20%
2	Slightly significant increase	68.03	0.89%
3	Significant increase	447.88	5.83%
4	Highly significant increase	1404.23	18.27%

3.3. Spatial Correlation Analysis of EEQ

3.3.1. Global Spatial Autocorrelation Analysis of RSEI

As depicted in Table 3, the Morans' I values for the Yanhe watershed are consistently positive, exceeding the threshold of 0, with associated *p*-values significantly below the 0.01 level. This statistical outcome underscores the pronounced spatial autocorrelation present in the remote-sensing-based ecological index (RSEI) across the study period. The Z-scores, surpassing the critical value of 2.58, provide robust evidence against the null hypothesis, confirming the non-random agglomeration of high and low RSEI values in the spatial distribution.

Upon examining the temporal trajectory of the RSEI spatial agglomeration, it is observed that this pattern has intensified over the two-decade span, with a particularly notable increase in 2010. This enhanced agglomeration in 2010 may be attributed to several factors unique to the Yanhe watershed. The implementation of ecological restoration

projects, such as the Grain-for-Green and the Gully Land Consolidation initiative, has led to significant reforestation efforts, particularly in the southern mountainous regions. These efforts have contributed to the formation of high RSEI clusters, indicative of improved ecological quality.

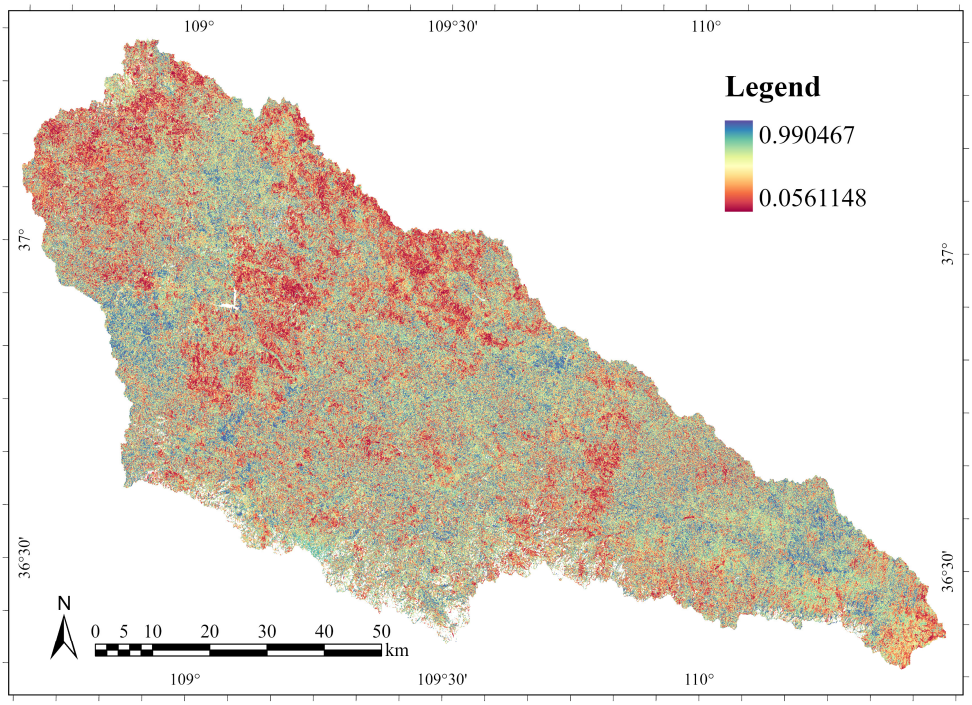


Figure 7. Hurst Exponent of RSEI change in Yanhe watershed from 2000 to 2020.

As shown in Table 3, the Moran's I index is consistently larger than 0, and the *p*-values are <0.01, indicating that the RSEI presents a significant spatial autocorrelation. The Z-scores are all greater than 2.58, indicating that the null hypothesis cannot be accepted, and the ecological index has an agglomeration state in the spatial distribution. From the long-term series, the spatial agglomeration of the RSEI in the Yanhe watershed is enhanced as a whole, and the agglomeration is higher in 2010.

Table 3. Global Moran's I and Local Moran's I index statistics of RSEI of Yanhe watershed in 2000, 2010, and 2020.

Year	Global Moran's I			Local Moran's I		
	Moran's I	Z-Core	*p*-Value	General G	Z-Core	*p*-Value
2000	0.18	30.89	0.00	0.0006	22.29	0.00
2010	0.32	55.75	0.00	0.0006	39.35	0.00
2020	0.21	36.70	0.00	0.0006	21.77	0.00

3.3.2. Local Spatial Autocorrelation Analysis of RSEI

Anselin Local Moran's I statistics serves for identifying hot spots, cold spots, and spatial outliers with statistical significance. As shown in Table 3, the *p*-value < 0.01, and the Z-value score > 2.58, so there are local high-value clustering characteristics. The spatial–temporal distribution features exhibited by the RSEI in the Yanhe watershed can be understood more clearly by examining the LISA map created by the local autocorrelation analysis.

(1) Temporal dynamics and spatial agglomeration

The LISA map, a product of the local autocorrelation analysis, offers a nuanced perspective on the spatial–temporal distribution of the RSEI. The years 2000, 2010, and 2020 each exhibit distinct high–high (H–H) and low–low (L–L) cluster areas within the Yanhe watershed, signifying significant positive spatial correlation and agglomeration patterns. Notably, there is considerable fluctuation in the extent of these clusters across the three periods. The H–H clusters increased by 219 grid cells from 2000 to 2010, and then decreased by 154 by 2020. Similarly, the L–L clusters saw an initial rise from 187 in 2000 to 367 in 2010, followed by a decline to 251 by 2020 (Figure 8).

(2) Spatial distribution and ecological stability

The Morans' I scatter diagram for the years 2000, 2010, and 2020, as shown in Figure 9, provides a dynamic view of how these spatial patterns have evolved over time. It is evident that the H–H clusters have fluctuated, with some areas showing a consolidation of high ecological quality, while others have experienced a decline. Similarly, the L–L clusters have shifted, reflecting the impact of human activities and environmental changes on the ecological landscape of the Yanhe watershed.

The H–H clusters, particularly in the Ziwu Mountains region of the southern Yanhe watershed, demonstrate relative stability, with a notable expansion northward in 2010 and a subsequent retraction by 2020, aligning with downstream areas (Figure 10). This area belongs to the interlaced transition zone of the forest belt and grassland belt. There are natural forests in the southern mountainous area, and the ecological environment is relatively stable. In the north, the dam land and river valley are mostly distributed near cities and towns. Human activities are frequent, soil organic matter content is low, vegetation coverage is low, and the RSEI shows a decreasing trend during the study period. In contrast, the L–L clusters, initially confined to a small area in the southern foothills of the Baiyu Mountains in 2000, expanded significantly by 2010, particularly in the urban development zones of Ansai District and Baota District. By 2020, two substantial L–L clusters emerged in the upper and middle reaches of the watershed.

(3) North–South Differentiation and Human Impact

The overall scale of H–H and L–L cluster values has increased, with significant fluctuations highlighting a pronounced north–south differentiation pattern. This pattern is especially evident in the upstream and middle reaches, where human activities are prevalent. The Grain-for-Green (GFG) program has played a role in shaping these patterns; however, urban development and construction activities have also exerted considerable influence. The interplay between ecological restoration efforts and urbanization presents a complex scenario, with the temporal fluctuation and spatial heterogeneity of EEQ cluster values reflecting this dynamic. The restoration efforts have led to increased vegetation cover and improved water retention capabilities, enhancing the ecological environment.

The natural topography and hydrological features of the Yanhe watershed also play a crucial role in shaping the LISA map patterns. Regions with a complex terrain and higher elevations, such as the southern mountainous areas, tend to have more stable ecological conditions, contributing to the persistence of H–H clusters. The semi-arid climate of the Loess Plateau, characterized by variable precipitation patterns, influences the distribution of ecological quality [6]. Areas receiving more consistent rainfall tend to support better vegetation growth, while those experiencing higher evaporation rates due to temperature variations show signs of ecological stress. The implementation of environmental policies, such as the Three-North Shelterbelt Project, has led to afforestation efforts that are visible in the expansion of H–H clusters [37]. However, the effectiveness of these policies can vary across different regions, influenced by local enforcement and adherence [5].

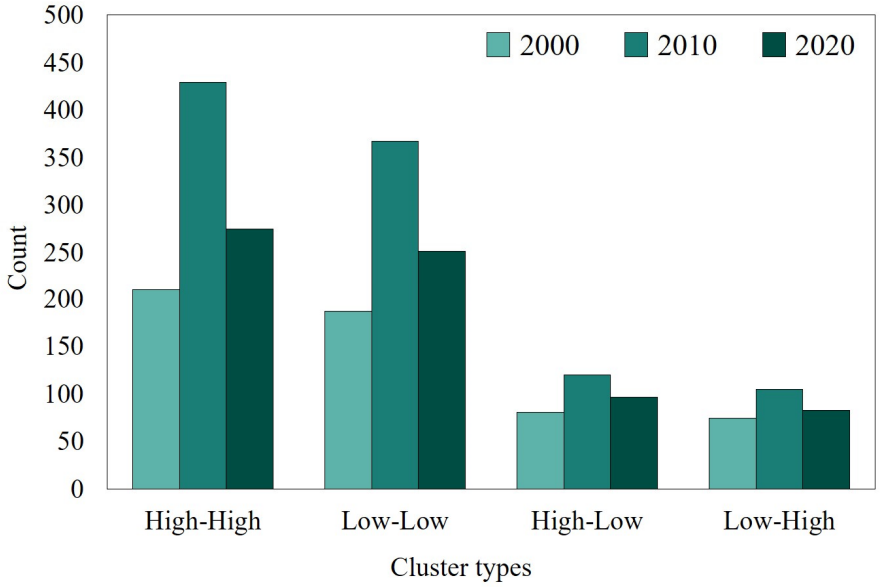


Figure 8. RSEI spatial clustering statistics for 2000, 2010, and 2020.

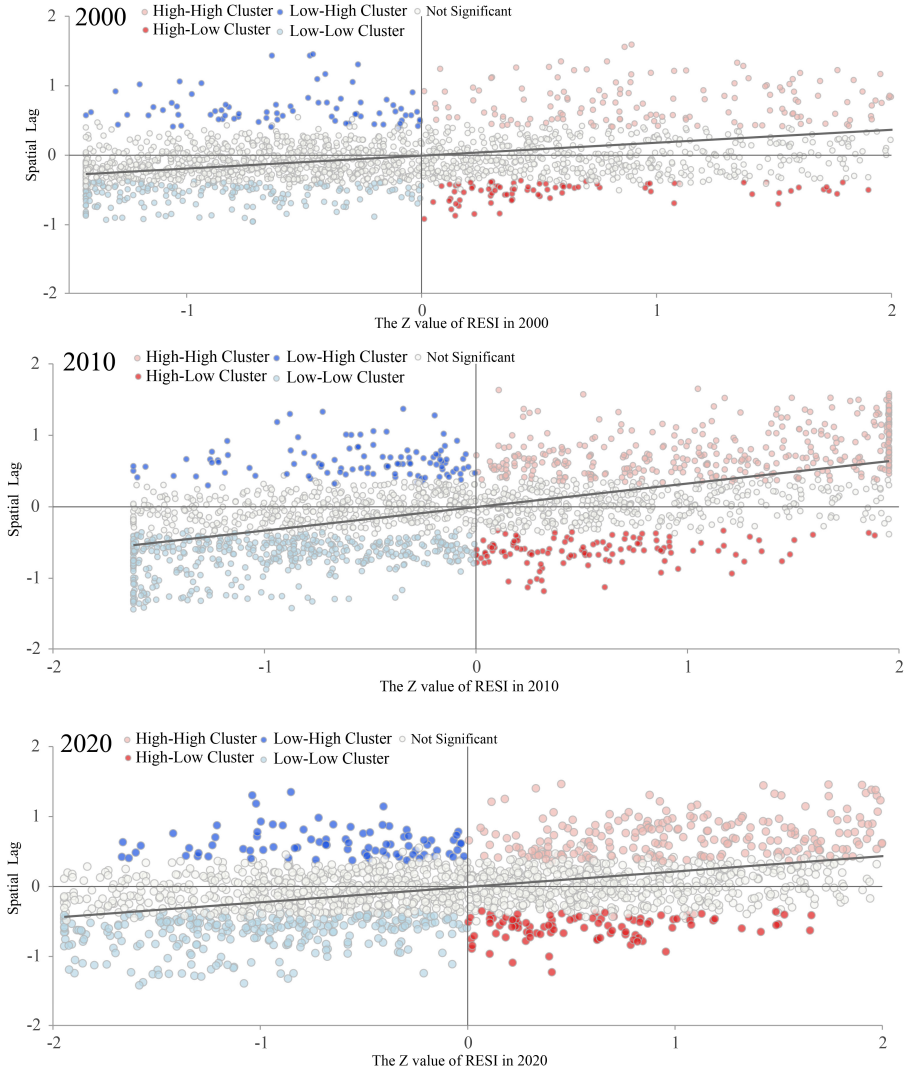


Figure 9. Moran's I scatter diagram of RSEI in 2000, 2010, and 2020.

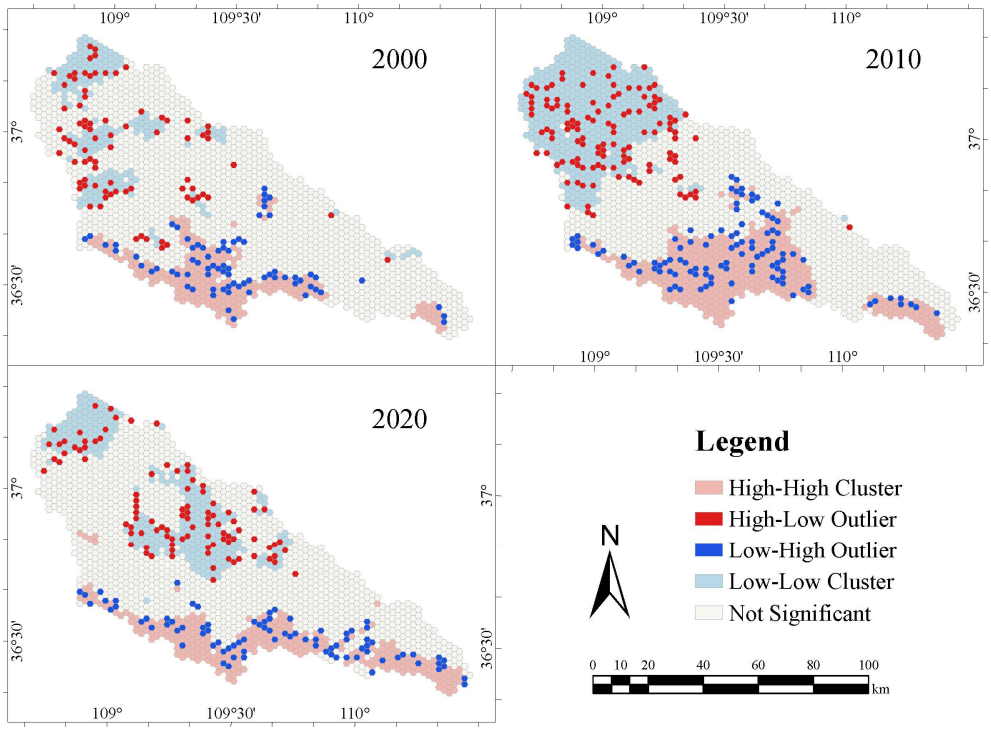


Figure 10. LISA map of RSEI local spatial cluster analysis in Yanhe watershed in 2000, 2010, and 2020.

4. Discussion

4.1. Influencing Factors and Applicability of RSEI

In this study, we observed significant temporal evolution and spatial heterogeneity in the ecological environment quality (EEQ) of the Yanhe watershed. To delve deeper into the causes of these observed patterns, we must consider the complex interplay between climate change, human activities, and the inherent ecological processes of the region. Climate variability, particularly changes in precipitation and temperature patterns, have been primary drivers of ecological fluctuations, affecting vegetation growth and water availability [42]. Additionally, human activities, such as land use changes, agricultural practices, and urbanization, have significantly altered the landscape, leading to variations in EEQ [54,55]. The zoning of land for different uses, as well as the implementation of ecological restoration programs like the Grain-for-Green and Gully Land Consolidation initiatives, have contributed to the observed improvements in certain areas, while some areas still struggle with the effects of past land degradation [56]. The complex interplay of these numerous factors has resulted in spatial heterogeneity and temporal lags in the ecological environment quality of the Yanhe watershed.

Our results show that for the Yanhe watershed, greenness and wetness had a positive impact on RSEI, while dryness and heat had a negative impact, which not only were consistent with the ecological background of semi-arid climate conditions and uneven temporal and spatial distribution of water resource, but also suggested a similar result to previous studies [22,57]. Notably, the WET index exhibited a higher contribution relative to NDVI in the RSEI calculation for the Yanhe watershed. This can be attributed to the region's' semi-arid climatic conditions and the spatial heterogeneity of local thermal and moisture conditions caused by the complex terrain and landforms [58]. Generally, water availability is a critical determinant of EEQ in such regions. The WET index's' sensitivity to changes in soil moisture and surface water dynamics reflects the essential role of water in supporting the regions' biodiversity and agricultural activities [59]. Leveraging the seasonality of precipitation patterns and the potential of effective water resource management practices may have further contributed to the prominence of the WET index in maintaining and enhancing the favorable ecological environment within the Yanhe watershed [60].

Considering the RSEI application stability, the average RSEI value in the Yanhe watershed over the past 20 years is approximately 0.46. This value can be compared to the results of 0.7 in islands [61], 0.6 in coastal cities [62,63], about 0.1 in arid wetlands [57], and 0.3 in urban areas [64]. The Yanhe watershed falls into the category of medium EEQ, which aligns with the current ecological environment status in each area. Therefore, the RSEI effectively reflects the EEQ in different regions.

4.2. Future EEQ Trends and Related Factors in Yanhe Watershed

We further superimposed the Sen + Mann–Kendall result on the Hurst Exponent result to obtain Figure A1 and Table A1. As can be seen from Table A1, the RSEI that will continue to increase in the future accounts for 23.57%, which is distributed in the entire Yanhe watershed (Figure A1), far higher than the 2.15% that will continue to decrease. Therefore, the overall ecological environment quality of the Yanhe watershed will continue to improve in the future. The area of the RSEI that will remain unchanged is 4686.62 km^2, accounting for 62.94%. And it is worth noting that some of them are concentrated in the southern mountain area, which is also the area with a high RSEI. Due to the good long-term vegetation development, it is conducive to the sustainability of ecological environment health [65,66]. However, in the north of the Yanhe watershed, a low RSEI will accumulate and remain unchanged in the future, which is closely related to the current hydrological conditions. This region is an area with a high runoff and sediment yield [55], and the landscape pattern changes are more complex [67], resulting in a lower ecological and environmental quality. The area where the RSEI continues to decrease is located in the center of the Yanhe watershed, where human activities are intensive and urban development and construction activities are frequent. As can be seen from Figure A1, although the ecological environment quality in the urban part of Baota District has been improved, there are still areas with *H* inconsistency, and there are great differences in both time and space, and the ecological environment quality is still unstable [68].

4.3. Limitations of RSEI and Suggestions for Future

Given the challenges associated with data acquisition and the dynamic nature of research advancements, it is important to acknowledge the limitations of this study, which will be further explored in the future. Firstly, the adoption of the RSEI as a representation of the EEQ in the Yanhe watershed is aligned with the geographical and climatic characteristics of the Loess Plateau. However, it is essential to recognize that the watershed's ecological system is highly intricate, subject to constant changes, and influenced by numerous uncertain factors, including governmental organizational management capacity, human behavioral patterns, and the impacts of climate change. In contrast to the conventional evaluation of EEQ with a single index, this study employed four crucial indicators encompassing Greenness, Wetness, Dryness, and Heat to comprehensively evaluate the Yanhe watershed, obtaining reasonable results. However, the inclusion of other diverse spatial data could provide a more nuanced understanding of the ecosystem. Examples of such data include land use patterns [40,69], carbon storage dynamics [36,70], and NPP [71]. Integrating these additional variables would contribute to a more comprehensive and holistic evaluation of the EEQ.

From the perspective of space governance, future research can further analyze the factors and mechanisms influencing EEQ at various spatial and temporal scales, thereby providing guidance for rational spatial governance. Developing a robust spatiotemporal management model is crucial to enable effective decision-making processes that can better integrate local planning initiatives and address the specific challenges presented by varying spatial scales. This comprehensive approach would facilitate a balanced and contextually appropriate solution for managing ecological issues. In additional, although ecological space restoration can be conducted using the results obtained from evaluating the EEQ through the RSEI, it is still unstable with large spatial differences and a fragile ecology in some local places. Therefore, in the future, ecological networks [23] can be constructed

and an ecological security pattern [71] implemented, which can enhance the stability and sustainability of the watershed.

5. Conclusions

The ecological environment quality (EEQ) of the Yanhe watershed, a microcosm of the Loess Plateau, has been under intense scrutiny due to its ecological significance and the challenges posed by climate change and human activities. This study presents a multi-temporal and spatial scale analytical framework, utilizing a 21-year span of remote sensing data via Google Earth Engine (GEE) and ArcGIS platforms. Our approach, scaling from pixel to grid analysis, was employed to assess the spatiotemporal dynamics of EEQ, underscored by the RSEI.

The comprehensive assessment, integrating raster trend analysis and the Hurst Exponent calculation, reveals an overall positive trend in the Yanhe watersheds' EEQ over the past two decades, with 72.48% of the area exhibiting minimal change. Significantly, the Hurst Exponent reveals a positive trend persistence, supported by 88.6% of the watershed area exhibiting values exceeding 0.5, which implies a future trajectory of EEQ that aligns with the studys' observed period. Spatial analysis has exposed significant positive spatial correlations in RSEI values across the benchmark years of 2000, 2010, and 2020. The presence of high–high (H–H) clusters, especially in the southern Ziwu Mountains, and low–low (L–L) clusters in urban development zones reflects the interplay between ecological conditions and human interventions. These patterns reflect socio-economic development and the impacts of key ecological policies, such as the Three-North Shelter Forest Program, Grain-for-Green (GFG), and Gully Land Consolidation (GLG) initiatives.

This study underscores the imperative for multi-scale, multi-period ecological assessments, which are indispensable for formulating efficacious ecological restoration and sustainability strategies. The positive trends observed, along with the spatial patterns identified, suggest that current ecological policies are yielding measurable improvements. The data indicate that a significant portion of the watershed has maintained stability, and the persistent positive trend suggests a continued trajectory of ecological enhancement. However, it is imperative to continue monitoring and to implement adaptive management strategies to ensure the sustainability of these improvements in the face of ongoing climate change and human activities. The insights from the Yanhe watershed contribute to the scientific understanding of ecological dynamics within the Loess Plateau and offer a robust model for ecological quality assessment applicable to similar environmental contexts.

Author Contributions: L.Z.: writing—original draft, software, visualization, and methodology. Q.H.: funding acquisition, project administration, and writing—review and editing. Y.D.: visualization and software. S.M.: resources. All authors have read and agreed to the published version of the manuscript.

Funding: This work was supported by the National Natural Science Foundation of China [grant number 52178030]; the National Key Research and Development Program [grant number 2022YFC3802803]; and the Fundamental Research Funds for the Central Universities, CHD [grant number 300102412723].

Data Availability Statement: The data will be made available upon request. The data are not publicly available due to the fact that they are part of ongoing research and are protected to ensure the integrity of our work and to respect the proprietary interests of the research team.

Acknowledgments: We are thankful to the anonymous reviewers for their valuable comments.

Conflicts of Interest: The authors declare that they have no known competing financial interests or personal relationships that could have appeared to influence the work reported in this paper.

Appendix A

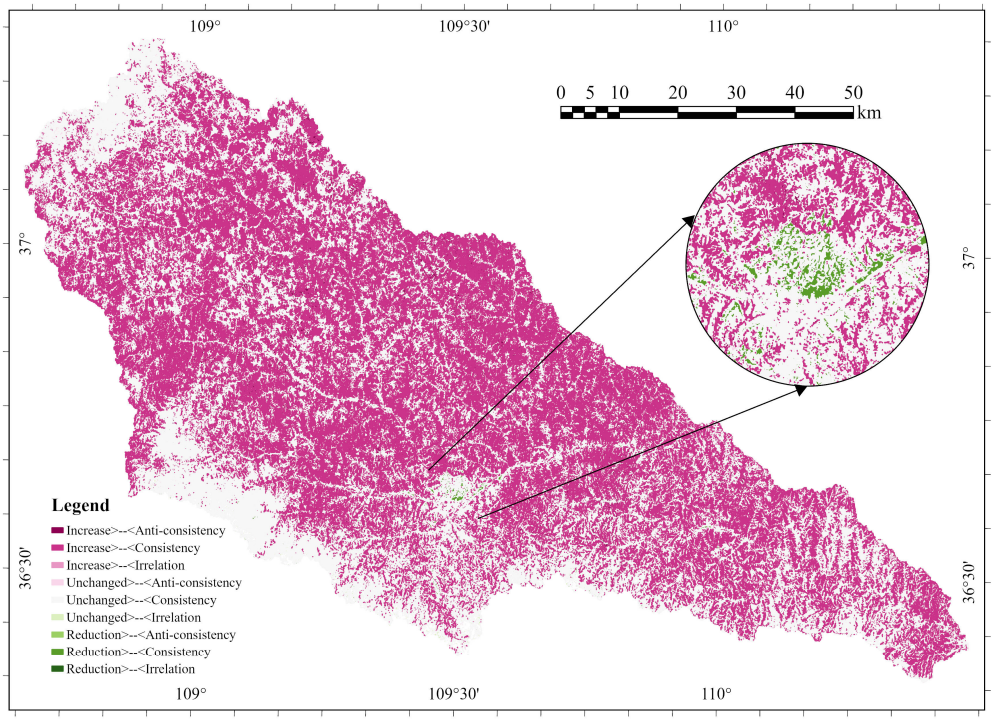


Figure A1. Spatial distribution of RSEI variation types in Yanhe watershed.

Table A1. Statistical table of RSEI variation types in Yanhe watershed.

Type of Change	Area (km^2)	Proportion (%)
Reduction>--<Anti-consistency	16.48	0.22%
Reduction>--<Irrelation	0.45	0.01%
Reduction>--<Consistency	160.41	2.15%
Unchanged>--<Anti-consistency	606.14	8.14%
Unchanged>--<Irrelation	22.10	0.30%
Unchanged>--<Consistency	4686.62	62.94%
Increase>--<Anti-consistency	193.86	2.60%
Increase>--<Irrelation	5.15	0.07%
Increase>--<Consistency	1755.43	23.57%

References

1. Crutzen, P.J. Geology of mankind. *Nature* **2002**, *415*, 23. [CrossRef] [PubMed]
2. Coseo, P.; Larsen, L. How factors of land use/land cover, building configuration, and adjacent heat sources and sinks explain Urban Heat Islands in Chicago. *Landsc. Urban Plan.* **2014**, *125*, 117–129. [CrossRef]
3. Qiao, Z.; Liu, L.; Qin, Y.; Xu, X.; Wang, B.; Liu, Z. The impact of urban renewal on land surface temperature changes: A case study in the main city of Guangzhou, China. *Remote Sens.* **2020**, *12*, 794. [CrossRef]
4. Jiang, Y.; Zevenbergen, C.; Ma, Y. Urban pluvial flooding and stormwater management: A contemporary review of China's challenges and "sponge cities" strategy. *Environ. Sci. Policy* **2018**, *80*, 132–143. [CrossRef]
5. Li, Y.; Zhang, X.; Cao, Z.; Liu, Z.; Lu, Z.; Liu, Y. Towards the progress of ecological restoration and economic development in China's Loess Plateau and strategy for more sustainable development. *Sci. Total Environ.* **2021**, *756*, 143676. [CrossRef] [PubMed]
6. Fu, B.; Liu, Y.; Lv, Y.; He, C.; Zeng, Y.; Wu, B. Assessing the soil erosion control service of ecosystems change in the Loess Plateau of China. *Ecol. Complex.* **2011**, *8*, 284–293. [CrossRef]
7. Kang, Y.; Gao, J.; Shao, H.; Zhang, Y.; Li, J.; Gao, Z. Evaluating the flow and sediment effects of gully land consolidation on the Loess Plateau, China. *J. Hydrol.* **2021**, *600*, 126535. [CrossRef]
8. Feng, X.; Fu, B.; Piao, S.; Wang, S.; Ciais, P.; Zeng, Z.; Lv, Y.; Zeng, Y.; Li, Y.; Jiang, X.; et al. Revegetation in China's Loess Plateau is approaching sustainable water resource limits. *Nat. Clim. Chang.* **2016**, *6*, 1019–1022. [CrossRef]
9. Wang, Z.; Fu, B.; Wu, X.; Li, Y.; Feng, Y.; Wang, S.; Wei, F.; Zhang, L. Vegetation resilience does not increase consistently with greening in China's Loess Plateau. *Commun. Earth Environ.* **2023**, *4*, 336. [CrossRef]

10. Jiang, W.; Fu, B.; Lü, Y. Assessing Impacts of Land Use/Land Cover Conversion on Changes in Ecosystem Services Value on the Loess Plateau, China. *Sustainability* **2020**, *12*, 7128. [CrossRef]
11. Guo, Y.; Wanf, N.; Chu, X.; Li, C.; Luo, X.; Feng, H. Analyzing vegetation coverage changes and its reasons on the Loess Plateau based on Google Earth Engine. *China Environ. Sci.* **2019**, *39*, 4804–4811. [CrossRef]
12. Shi, M.; Lin, F.; Jing, X.; Li, B.; Shi, Y.; Hu, Y. Ecological Environment Quality Assessment of Arid Areas Based on Improved Remote Sensing Ecological Index—A Case Study of the Loess Plateau. *Sustainability* **2023**, *15*, 13881. [CrossRef]
13. Yang, X.; Bai, Y.; Che, L.; Qiao, F.; Xie, L. Incorporating ecological constraints into urban growth boundaries: A case study of ecologically fragile areas in the Upper Yellow River. *Ecol. Indic.* **2021**, *124*, 107436. [CrossRef]
14. Xu, H. A remote sensing index for assessment of regional ecological changes. *China Environ. Sci.* **2013**, *33*, 889–897. (In Chinese) [CrossRef]
15. Zhang, J.; Yang, G.; Yang, L.; Li, Z.; Gao, M.; Yu, C.; Gong, E.; Long, H.; Hu, H. Dynamic monitoring of environmental quality in the Loess Plateau from 2000 to 2020 using the Google Earth Engine platform and the remote sensing ecological index. *Remote Sens.* **2022**, *14*, 5094. [CrossRef]
16. Huang, S.; Tang, L.; Hupy, J.P.; Wang, Y.; Shao, G. A commentary review on the use of normalized difference vegetation index (NDVI) in the era of popular remote sensing. *J. For. Res.* **2021**, *32*, 1–6. [CrossRef]
17. Reinermann, S.; Asam, S.; Kuenzer, C. Remote sensing of grassland production and management—A review. *Remote Sens.* **2020**, *12*, 1949. [CrossRef]
18. Xiao, J.; Chevallier, F.; Gomez, C.; Guanter, L.; Hicke, J.A.; Huete, A.R.; Ichii, K.; Ni, W.; Pang, Y.; Rahman, A.F.; et al. Remote sensing of the terrestrial carbon cycle: A review of advances over 50 years. *Remote Sens. Environ.* **2019**, *233*, 111383. [CrossRef]
19. Pham, T.D.; Yokoya, N.; Bui, D.T.; Yoshino, K.; Friess, D.A. Remote sensing approaches for monitoring mangrove species, structure, and biomass: Opportunities and challenges. *Remote Sens.* **2019**, *11*, 230. [CrossRef]
20. Jiménez-Muñoz, J.C.; Sobrino, J.A.; Skoković, D.; Mattar, C.; Cristóbal, J. Land surface temperature retrieval methods from Landsat-8 thermal infrared sensor data. *IEEE Geosci. Remote Sens. Lett.* **2014**, *11*, 1840–1843. [CrossRef]
21. Xiong, Y.; Xu, W.; Lu, N.; Huang, S.; Wu, C.; Wang, L.; Dai, F.; Kou, W. Assessment of spatial–temporal changes of ecological environment quality based on RSEI and GEE: A case study in Erhai Lake Basin, Yunnan province, China. *Ecol. Indic.* **2021**, *125*, 107518. [CrossRef]
22. Yuan, B.; Fu, L.; Zou, Y.; Zhang, S.; Chen, X.; Li, F.; Deng, Z.; Xie, Y. Spatiotemporal change detection of ecological quality and the associated affecting factors in Dongting Lake Basin, based on RSEI. *J. Clean. Prod.* **2021**, *302*, 126995. [CrossRef]
23. Yang, L.; Suo, M.; Gao, S.; Jiao, H. Construction of an ecological network based on an integrated approach and circuit theory: A case study of Panzhou in Guizhou Province. *Sustainability* **2022**, *14*, 9136. [CrossRef]
24. Attaur, R.; Dawood, M. Spatio-statistical analysis of temperature fluctuation using Mann–Kendall and Sen's slope approach. *Clim. Dyn.* **2017**, *48*, 783–797. [CrossRef]
25. Meng, X.; Gao, X.; Li, S.; Lei, J. Spatial and temporal characteristics of vegetation NDVI changes and the driving forces in Mongolia during 1982–2015. *Remote Sens.* **2020**, *12*, 603. [CrossRef]
26. Liu, S.; Li, W.; Qiao, W.; Wang, Q.; Hu, Y.; Wang, Z. Effect of natural conditions and mining activities on vegetation variations in arid and semiarid mining regions. *Ecol. Indic.* **2019**, *103*, 331–345. [CrossRef]
27. Peng, J.; Liu, Z.; Liu, Y.; Wu, J.; Han, Y. Trend analysis of vegetation dynamics in Qinghai–Tibet Plateau using Hurst Exponent. *Ecol. Indic.* **2012**, *14*, 28–39. [CrossRef]
28. Hurst, H.E. Long-term storage capacity of reservoirs. *Trans. Am. Soc. Civ. Eng.* **1951**, *116*, 770–799. [CrossRef]
29. Geng, W.; Li, Y.; Zhang, P.; Yang, D.; Jing, W.; Rong, T. Analyzing spatio-temporal changes and trade-offs/synergies among ecosystem services in the Yellow River Basin, China. *Ecol. Indic.* **2022**, *138*, 108825. [CrossRef]
30. Jiang, L.; Jiapaer, G.; Bao, A.; Guo, H.; Ndayisaba, F. Vegetation dynamics and responses to climate change and human activities in Central Asia. *Sci. Total Environ.* **2017**, *599–600*, 967–980. [CrossRef]
31. Fan, C.; Myint, S. A comparison of spatial autocorrelation indices and landscape metrics in measuring urban landscape fragmentation. *Landsc. Urban Plan.* **2014**, *121*, 117–128. [CrossRef]
32. Hu, X.; Xu, H. A new remote sensing index for assessing the spatial heterogeneity in urban ecological quality: A case from Fuzhou City, China. *Ecol. Indic.* **2018**, *89*, 11–21. [CrossRef]
33. Wang, F.; Li, W.-H.; Lin, Y.-M.; Nan, X.-X.; Hu, Z.-R. Spatiotemporal pattern and driving force analysis of ecological environmental quality in typical ecological areas of the Yellow River Basin from 1990 to 2020. *Environ. Sci.* **2023**, *44*, 2518–2527. [CrossRef] [PubMed]
34. Yang, H.; Yu, J.; Xu, W.; Wu, Y.; Lei, X.; Ye, J.; Geng, J.; Ding, Z. Long-time series ecological environment quality monitoring and cause analysis in the Dianchi Lake Basin, China. *Ecol. Indic.* **2023**, *148*, 110084. [CrossRef]
35. Ren, K.; Luo, M.; Zhao, Y.; Han, L.; Zhang, L.; Yang, S. Evaluation of ecological environment and urban development quality in Xi'an City, China. *Chin. J. Appl. Ecol.* **2022**, *33*, 2485–2492. [CrossRef] [PubMed]
36. Tang, P.; Huang, J.; Zhou, H.; Fang, C.; Zhan, Y.; Huang, W. Local and telecoupling coordination degree model of *urbanization* and the eco-environment based on RS and GIS: A case study in the Wuhan urban agglomeration. *Sustain. Cities Soc.* **2021**, *75*, 103405. [CrossRef]
37. Wei, C.; Zhou, Y.; Zhu, F.; Song, Z. Spatial and temporal evolution characteristics of ecological environment quality in Shizuishan region based on GEE. *Eng. Surv. Mapp.* **2023**, *32*, 30–39. (In Chinese) [CrossRef]

38. Geng, J.; Yu, K.; Xie, Z.; Zhao, G.; Ai, J.; Yang, L.; Yang, H.; Liu, J. Analysis of spatiotemporal variation and drivers of ecological quality in Fuzhou based on RSEI. *Remote Sens.* **2022**, *14*, 4900. [CrossRef]
39. Su, C.; Fu, B.; Wei, Y.; Lv, Y.; Liu, G.; Wang, D.; Mao, K.; Feng, X. Ecosystem management based on ecosystem services and human *activities*: A case study in the Yanhe watershed. *Sustain. Sci.* **2012**, *7*, 17–32. [CrossRef]
40. Zhou, H.; Van Rompaey, A.; Wang, J. Detecting the impact of the "Grain for Green" program on the mean annual vegetation cover in the Shaanxi province, China using SPOT-VGT NDVI data. *Land Use Policy* **2009**, *26*, 954–960. [CrossRef]
41. Deng, Y.; Wang, S.; Bai, X.; Luo, G.; Wu, L.; Chen, F.; Wang, J.; Li, C.; Yang, Y.; Hu, Z.; et al. Vegetation greening intensified soil drying in some semi-arid and arid areas of the world. *Agric. For. Meteorol.* **2020**, *292–293*, 108103. [CrossRef]
42. Bai, M.; Mo, X.; Liu, S.; Hu, S. Contributions of climate change and vegetation greening to evapotranspiration trend in a typical hilly-gully basin on the Loess Plateau, China. *Sci. Total Environ.* **2019**, *657*, 325–339. [CrossRef] [PubMed]
43. Xu, H. Modification of normalised difference water index (NDWI) to enhance open water features in remotely sensed imagery. *Int. J. Remote Sens.* **2007**, *27*, 3025–3033. [CrossRef]
44. Fu, J.; Zhang, S. Functional assessment and coordination characteristics of production, living, ecological function—A case study of Henan Province, China. *Int. J. Environ. Res. Public Health* **2021**, *18*, 8051. [CrossRef] [PubMed]
45. Birch, C.P.D.; Oom, S.P.; Beecham, J.A. Rectangular and hexagonal grids used for observation, experiment and simulation in ecology. *Ecol. Model.* **2007**, *206*, 347–359. [CrossRef]
46. Xu, H. A new index for delineating built-up land features in satellite imagery. *Int. J. Remote Sens.* **2008**, *29*, 4269–4276. [CrossRef]
47. Crist, E.P. A TM Tasseled Cap equivalent transformation for reflectance factor data. *Remote Sens. Environ.* **1985**, *17*, 301–306. [CrossRef]
48. Chen, C.; Bu, J.; Zhang, Y.; Zhuang, Y.; Chu, Y.; Hu, J.; Guo, B. The application of the tasseled cap transformation and feature knowledge for the extraction of coastline information from remote sensing images. *Adv. Space Res.* **2019**, *64*, 1780–1791. [CrossRef]
49. Huang, C.; Wylie, B.K.; Yang, L.; Homer, C.G.; Zylstra, G. Derivation of a tasselled cap transformation based on Landsat 7 at-satellite reflectance. *Int. J. Remote Sens.* **2002**, *23*, 1741–1748. [CrossRef]
50. Nichol, J. Remote sensing of urban heat islands by day and night. *Photogramm. Eng. Remote Sens.* **2005**, *71*, 613–622. [CrossRef]
51. Sen, P.K. Estimates of the regression coefficient based on Kendall's Tau. *J. Am. Stat. Assoc.* **1968**, *63*, 1379–1389. [CrossRef]
52. Mann, H.B. Nonparametric tests against trend. *Econometrica* **1945**, *13*, 245–259. [CrossRef]
53. Kendall, M.G. *Rank Correlation Methods*; Charles Griffin and Company, Ltd.: London, UK, 1949.
54. Sun, Z.; Han, J.; Li, Y.; Yang, L.; Shi, L.; Yan, J. Effects of large-scale land consolidation projects on ecological environment quality: A case study of a land creation project in Yan'an, China. *Environ. Int.* **2024**, *183*, 108392. [CrossRef] [PubMed]
55. Yang, X.; Sun, W.; Li, P.; Mu, X.; Gao, P.; Zhao, G. Integrating agricultural land, water yield and soil conservation trade-offs into spatial land use planning. *Ecol. Indic.* **2019**, *104*, 219–228. [CrossRef]
56. Yang, S.; Zhao, W.; Liu, Y.; Wang, S.; Wang, J.; Zhai, R. Influence of land use change on the ecosystem service trade-offs in the ecological restoration area: Dynamics and scenarios in the Yanhe watershed, China. *Sci. Total Environ.* **2018**, *644*, 556–566. [CrossRef]
57. Jing, Y.; Zhang, F.; He, Y.; Kung, H.-T.; Johnson, V.C.; Arikena, M. Assessment of spatial and temporal variation of ecological environment quality in Ebinur Lake Wetland National Nature Reserve, Xinjiang, China. *Ecol. Indic.* **2020**, *110*, 105874. [CrossRef]
58. Yang, Q.; Fan, J.; Luo, Z. Response of soil moisture and vegetation growth to precipitation under different land uses in the Northern Loess Plateau, China. *CATENA* **2024**, *236*, 107728. [CrossRef]
59. Wei, S.; Jin, X.; Jie, R.; Wang, Y.; Xu, Z.; Fan, Y.; Gu, Z.; Hong, C.; Lin, J.; Zhou, Y. Ecological environment quality assessment based on remote sensing data for land consolidation. *J. Clean. Prod.* **2019**, *239*, 118126. [CrossRef]
60. Zhang, L.; Dawes, W.; Walker, G. Response of mean annual evapotranspiration to vegetation changes at catchment scale. *WRR* **2001**, *37*, 701–708. [CrossRef]
61. Liu, C.; Yang, M.; Hou, Y.; Zhao, Y.; Xue, X. Spatiotemporal evolution of island ecological quality under different urban densities: A comparative analysis of Xiamen and Kinmen Islands, southeast China. *Ecol. Indic.* **2021**, *124*, 107438. [CrossRef]
62. Zheng, Z.; Wu, Z.; Chen, Y.; Yang, Z.; Marinello, F. Exploration of eco-environment and urbanization changes in coastal zones: A case study in China over the past 20 years. *Ecol. Indic.* **2020**, *119*, 106847. [CrossRef]
63. Xu, H.; Wang, Y.; Guan, H.; Shi, T.; Hu, X. Detecting ecological changes with a remote sensing based ecological index (RSEI) produced time series and change vector analysis. *Remote Sens.* **2019**, *11*, 2345. [CrossRef]
64. Zhang, Y.; She, J.; Long, X.; Zhang, M. Spatio-temporal evolution and driving factors of eco-environmental quality based on RSEI in Chang-Zhu-Tan metropolitan circle, central China. *Ecol. Indic.* **2022**, *144*, 109436. [CrossRef]
65. Ni, Y.; Yu, Z.; Lv, X.; Ma, L.; Zhang, Q.; Wang, J. Response of runoff to vegetation change in typical basin of the Loess Plateau. *Ecol. Eng.* **2022**, *182*, 106704. [CrossRef]
66. Peng, S.; Yu, K.; Li, Z.; Wen, Z.; Zhang, C. Integrating potential natural vegetation and habitat suitability into revegetation programs for sustainable ecosystems under future climate change. *Agric. For. Meteorol.* **2019**, *269–270*, 270–284. [CrossRef]
67. Zhou, Z.; Li, J. The correlation analysis on the landscape pattern index and hydrological processes in the Yanhe watershed, China. *J. Hydrol.* **2015**, *524*, 417–426. [CrossRef]
68. Lian, Y.; Sun, M.; Wang, J.; Luan, Q.; Jiao, M.; Zhao, X.; Gao, X. Quantitative impacts of climate change and human activities on the runoff evolution process in the Yanhe River Basin. *Phys. Chem. Earth Parts A/B/C* **2021**, *122*, 102998. [CrossRef]

69. Yang, Z.; Sun, C.; Ye, J.; Gan, C.; Li, Y.; Wang, L.; Chen, Y. Spatio-temporal heterogeneity of ecological quality in Hangzhou Greater Bay Area (HGBA) of China and response to land use and cover change. *Remote Sens.* **2022**, *14*, 5613. [CrossRef]
70. Yang, Y.; Li, H.; Qian, C. Analysis of the implementation effects of ecological restoration projects based on carbon storage and eco-environmental quality: A case study of the Yellow River Delta, China. *J. Environ. Manag.* **2023**, *340*, 117929. [CrossRef]
71. Chen, S.; Zhang, Q.; Chen, Y.; Zhou, H.; Xiang, Y.; Liu, Z.; Hou, Y. Vegetation change and eco-environmental quality evaluation in the Loess Plateau of China from 2000 to 2020. *Remote Sens.* **2023**, *15*, 424. [CrossRef]

Disclaimer/Publisher's Note: The statements, opinions and data contained in all publications are solely those of the individual author(s) and contributor(s) and not of MDPI and/or the editor(s). MDPI and/or the editor(s) disclaim responsibility for any injury to people or property resulting from any ideas, methods, instructions or products referred to in the content.